

## Research Article

# Synthesis and Antibacterial, Antioxidant, and Molecular Docking Analysis of Some Novel Quinoline Derivatives

Digafie Zeleke,<sup>1</sup> Rajalakshmanan Eswaramoorthy ,<sup>1</sup> Zerihun Belay,<sup>2</sup> and Yadessa Melaku <sup>1</sup>

<sup>1</sup>Department of Applied Chemistry, Adama Science and Technology University, Adama, Ethiopia

<sup>2</sup>Department of Applied Biology, Adama Science and Technology University, Adama, Ethiopia

Correspondence should be addressed to Yadessa Melaku; [yadessamelaku2010@gmail.com](mailto:yadessamelaku2010@gmail.com)

Received 9 March 2020; Revised 8 June 2020; Accepted 19 June 2020; Published 24 July 2020

Academic Editor: Ponnurengam Malliappan Sivakumar

Copyright © 2020 Digafie Zeleke et al. This is an open access article distributed under the Creative Commons Attribution License, which permits unrestricted use, distribution, and reproduction in any medium, provided the original work is properly cited.

2-Chloroquinoline-3-carbaldehyde and 2-chloro-8-methylquinoline-3-carbaldehyde derivatives were synthesized through Vilsmeier formulation of acetanilide and N-(o-tolyl)acetamide. Aromatic nucleophilic substitution reaction was used to introduce various nucleophiles in place of chlorine under different reaction conditions. The carbaldehyde group was oxidized by permanganate method and reduced with metallic sodium in methanol and ethanol. The synthesized compounds were characterized by UV-Vis, IR, and NMR. The antibacterial activity of the synthesized compounds was screened against two Gram-positive bacteria (*Bacillus subtilis* ATCC6633 and *Staphylococcus aureus* ATCC25923) and two Gram-negative bacteria (*Escherichia coli* ATCC 25922 and *Pseudomonas aeruginosa* ATCC 27853). Most of the compounds displayed potent activity against two or more bacterial strains. Among them, compounds **6** and **15** showed maximum activity against *Pseudomonas aeruginosa* with mean inhibition zones of  $9.67 \pm 1.11$  and  $10.00 \pm 0.44$  mm, respectively, while ciprofloxacin showed mean inhibition zone of  $8.33 \pm 0.44$  mm at similar concentration. On the other hand, compound **8** exhibited maximum activity against *Escherichia coli* with inhibition zones of about  $9.00 \pm 0.55$  mm at  $300 \mu\text{g/mL}$  and  $11.33 \pm 1.11$  mm at  $500 \mu\text{g/mL}$ . The radical scavenging activity of these compounds was evaluated using 1,1-diphenyl-2-picrylhydrazyl (DPPH), and all of them displayed moderate antioxidant activity, with compound **7** exhibiting the strongest activity. The molecular docking study of the synthesized compounds was conducted to investigate their binding pattern with DNA gyrase, all of them were found to have minimum binding energy ranging from  $-6.0$  to  $-7.33$  kcal/mol, and the best result was achieved with compound **11**. The findings of the in vitro antibacterial and molecular docking analysis demonstrated that the synthesized compounds have potential of antibacterial activity and can be further optimized to serve as lead compounds.

## 1. Introduction

Antibacterial therapy has been challenging because of the alarming rate in rise of infections caused by bacteria coupled with their resistance to most of first-line antibiotic agents [1]. This is a serious threat to human health of the world in the 21<sup>st</sup> century and urgently calls continuing research to find out compounds possessing better antimicrobial with broad-spectrum activities. Hence, designing new drugs to treat disease and inflammations without causing significant side effects on patients is very important. In view of this,

quinoline derivatives are among important compounds previously reported to have a wide arrays of biological activities [2, 3]. Therefore, introduction of different functional groups on quinoline scaffold is a very good idea for the development of new drug.

The discovery of nalidixic acid in 1962, along with its introduction for clinical use in 1967, marks the beginning of decades of quinolone development and use [4]. Since then, various fluoroquinolones have been synthesized and used to treat various bacterial infections for decades [4]. However, currently some of them have been removed from market due

to intolerable side effects; in addition, some bacteria have also developed resistance against them and have narrowed their spectrum of activities [5].

In general, fluoroquinolones underwent four generations of development and improvement since the discovery of nalidixic acid, with each subsequent generation exhibiting broader and stronger bioactivity and less side effects than the previous one [5, 6]. Oxolinic acid, pipemidic acid, and nalidixic acid belong to the first generation and were used for the treatment of urinary tract infection caused by the majority of Gram-negative bacteria; however, all of them have short lifetime [6].

Enoxacin, ofloxacin, lomefloxacin, norfloxacin, and ciprofloxacin are in the second generation, have longer half-life, and improved activity against Gram-negative bacteria compared to the first generation [6, 7]. Sparfloxacin, grepafloxacin, and temafloxacin belong to the third generation [8] and are used as oral broad-spectrum antibacterial agents in the treatment of acute bacterial exacerbation of chronic bronchitis and mild-to-moderate pneumonia [9].

Gatifloxacin, clinafloxacin, trovafloxacin, and moxifloxacin belong to the fourth generation of fluoroquinolone drugs, which display extended activity against both Gram-negative and -positive bacteria strains; additionally, they are active against anaerobes and atypical bacteria [10].

Besides fluoroquinolone-based drugs, 2-chloroquinoline-3-carbaldehyde derivatives have also attracted much attention due to their considerable biological and pharmacological activities including antimicrobial [8], anti-inflammatory [11–13], antimalarial [14, 15], anticancer [16], antiviral [17, 18], and antifungal activities [19, 20]. Inspired by these reports, we have designed and synthesized various quinoline-3-carbaldehyde derivatives and evaluated their antibacterial and radical scavenging activities. Also incorporated herein is the *in silico* molecular docking analysis of the synthesized derivatives of quinolines.

## 2. Materials and Methods

**2.1. General.** Melting points were determined using open capillary tubes (Thiele) and were uncorrected. Analytical TLC was run on a 0.2 mm thick layer of silica gel GF<sub>254</sub> (Merck) on aluminum plate. Spots were detected using UV lamp. Column chromatography was performed using silica gel 60 (250–400 mesh) Merck. The IR spectra of compounds were recorded using a Perkin-Elmer BX Spectrometer (400–4000 cm<sup>-1</sup>) as KBr pellets. NMR spectra were recorded using Bruker Avance 400 spectrometer operating at 400 MHz using CDCl<sub>3</sub> and DMSO-d<sub>6</sub> as a solvent. All chemicals were purchased from Loba Chemie PVT, Ltd.

### 2.2. Chemistry

**2.2.1. Synthesis of Acetanilide (3).** In 250 mL round flask, aniline (20 mL), acetic anhydride (22 mL), zinc powder (0.2 g), and acetic acid (23 mL) were added. The mixture was boiled under reflux using water condenser for an hour. Then, it was cooled to room temperature and poured into 200 mL

of crushed ice water. The solid product was collected by suction filtration. White crystal; yield 69%, mp 112–113°C (Lit. mp 114.3°C).

**2.2.2. Synthesis of 2-Chloroquinoline-3-carbaldehyde (4).** N,N-dimethylformamide (20 mL, 0.26 mol) was added to a 100 mL round-bottom flask guarded with drying tube; it was cooled to 0°C using ice bath. Then, phosphorus oxychloride (70 mL, 0.75 mol) was added dropwise to it from dropping funnel guarded by drying tube while being stirred by magnetic stirrer. This addition was done for 30 minutes. Then acetamide (13.5 g, 0.1 mol) was added to it. After 5 minutes, the dropper funnel was replaced by air condenser with guarding tube at its end, and the mixture was heated for 22 hours on oil bath at 85–90°C. Then it was cooled to room temperature, poured into a beaker containing 400 mL crushed ice water, and stirred for 20 minutes. The yellow solid product was collected by suction filtration and washed with 100 mL cold water. The crude yield was 11.5 g (60%) and was recrystallized from ethyl acetate. yellow crystal; mp 146–148°C; yield 48.5%;  $R_f = 0.22$  (*n*-hexane:EtOAc = 9:1); UV-Vis (MeOH)  $\lambda_{max} = 280$  nm; IR (cm<sup>-1</sup>, KBr): 3035 (CH-arom.), 1693 (C=O aldehyde), 1621 (quinoline C=N str.), 599 (aromatic C=C str.); <sup>1</sup>H NMR (400 MHz, CDCl<sub>3</sub>)  $\delta_H$  7.65 (1H, m, H-6), 7.88 (1H, m, H-7), 7.97 (1H, d,  $J = 8.25$  Hz, H-8), 8.07 (1H, d,  $J = 8.25$  Hz, H-5), 8.74 (1H, s, H-4), and 10.54 (1H, s, H-9); <sup>13</sup>C NMR (100 MHz, CDCl<sub>3</sub>)  $\delta_C$  126.3 (C-1), 126.5 (C-8), 128.2 (C-6), 128.6 (C-4a), 129.7 (C-5), 133.6 (C-7), 140.3 (C-4), 149.6 (C-8a), 150.1 (C-2), and 189.1 (C-9).

**2.2.3. Synthesis of 2-Methoxyquinoline-3-carbaldehyde (5).** A 100 mL two-neck round-bottom flask was charged with methanol (10 mL), N,N-dimethylformamide (10 mL), 2-chloroquinoline-3-carbaldehyde (0.5 g, 0.0026 mol), and potassium carbonate (0.67 g, 0.0048 mol); the mixture was refluxed using water condenser for 6 hours; and the progress of reaction was monitored with TLC. After completion of the reaction, methanol was removed by distillation, allowed to cool to room temperature, and then added to 100 mL ice-cold water. The solid product was collected by fractional distillation and washed with excess ice-cold water. The amount of product was 0.44 g. Gray powder; yield 90.2%; mp 106–108°C;  $R_f = 0.32$  (*n*-hexane:EtOAc = 9:1); UV-Vis  $\lambda_{max}$  (MeOH) 295 nm; IR (cm<sup>-1</sup>, KBr): 3065.4 (aromatic C-H str.), 2919.3 (aliphatic C-H str.), 2847 (aliphatic C-H str.), 1673 (aldehyde C=O str.), 1620 (quinoline C=N str.), 1599 and 1579 (aromatic C=C str.); <sup>1</sup>H NMR (400 MHz, CDCl<sub>3</sub>)  $\delta_H$  4.22 (3H, s, H-10), 7.45 (1H, t,  $J = 7.3$  Hz, H-7), 7.76 (1H, t,  $J = 7.7$  Hz, H-6), 7.85 (2H, m, H-5, H-8), 8.60 (1H, s, H-4), and 10.49 (1H, s, H-9); <sup>13</sup>C NMR (100 MHz, CDCl<sub>3</sub>)  $\delta_C$  55.9 (C-10), 120.0 (C-3), 124.4 (C-6), 125.1 (C-4a), 127.1 (C-8), 129.8 (C-5), 132.6 (C-7), 140.0 (C-3), 149.0 C-8a), 161.2 (C-2), and 189.4 (C-9).

**2.2.4. Synthesis of 2-Ethoxyquinoline-3-carbaldehyde (6).** A 100 mL two-neck round-bottom flask was charged with 2-chloroquinoline-3-carbaldehyde (0.5 g, 0.0026 mol),

potassium carbonate (0.6 g, 0.0044 mol), ethanol (10 mL), and N,N-dimethylformamide (10 mL), and the necks were fitted with water condenser and stopper. The mixture was refluxed for 5 hours and the progress of the reaction was monitored with TLC. At the end, the ethanol was removed by distillation, and the remaining cooled mixture was poured into 100 mL crushed ice water. The solid mass was collected by suction filtration. Yield 67.3%; white powder; mp 63–65°C,  $R_f=0.38$  (*n*-hexane:EtOAc = 9:1), UV-Vis  $\lambda_{\max}$  (MeOH) 300 nm; IR ( $\text{cm}^{-1}$ , KBr) 3429 (OH str.), 3055 (aromatic C-H str.), 2930.9 (aliphatic C-H str.), 2874.45 (aliphatic C-H), 1683 (C=O str.), 1621 (quinoline C=N str.), 1589.6 and 1566 (aromatic C=C str.);  $^1\text{H}$  NMR (400 MHz,  $\text{CDCl}_3$ )  $\delta_{\text{H}}$  1.53 (3H, t,  $J_{12}=7.05$  Hz, H-11), 4.89 (2H, q,  $J_{12}=7.05$  Hz, H-10), 7.43 (1H, t,  $J=7.3$  Hz, H-7), 7.72 (1H, t,  $J=7.3$  Hz, H-6) 7.84 (2H, d,  $J=8.37$  Hz, H-8, H-5), 8.59 (1H, s, H-4), and 10.61 (1H, s, H-9);  $^{13}\text{C}$  NMR (100 MHz,  $\text{CDCl}_3$ )  $\delta_{\text{C}}$  14.5 (C-11), 62.4 (C-10) 120.0 (C-3), 124.3 (C-4a), 124.9 (C-6), 127.3 (C-8), 129.8 (C-5), 132.5 (C-7), 139.7 (C-4), 149.1 (C-8a), 161.2 (C-2), and 189.07 (C-9).

**2.2.5. Synthesis of 2-Thiocyanatoquinoline-3-carbaldehyde (7).** Potassium thiocyanate (0.24 g, 0.0024 mol), 2-chloro-8-methyl quinoline-3-carbaldehyde (0.5 g, 0.0024 mol), and potassium carbonate (0.65 g, 0.0047 mol) were added to 100 mL two-neck round-bottom flask containing N,N-dimethylformamide (20 mL). A water condenser was placed on one of its neck, and the other was closed with glass stopper and then refluxed for 3 hours, and the progress of the reaction was followed by TLC. The system was cooled to room temperature and poured into 50 mL crushed ice water. The solid product was collected with suction filtration and washed with 10 mL cold water. Yield 83.6%; orange powder; mp 134–136°C;  $R_f=0.44$  (*n*-hexane:EtOAc = 2:1); UV-Vis  $\lambda_{\max}$  (MeOH) 255 nm; IR ( $\text{cm}^{-1}$ , KBr) 3045 (aromatic C-H str.), 2919.9 (aliphatic C-H str.), 2182 (cyanide S-C $\equiv$ N str.), 1683 (aldehyde C=O str.), 1610 (quinoline C=N str.), 1572 (aromatic C=C str.), 1512 and 1340 (O=N-O str.);  $^1\text{H}$  NMR (400 MHz,  $\text{CDCl}_3$ )  $\delta_{\text{H}}$  7.50 (1H, d,  $J=7.8$  Hz, H-8), 7.61 (1H, d,  $J=8.9$  Hz, H6), 7.72 (1H, d,  $J=8.8$  Hz, H-7), 7.85 (1H, d,  $J=8.9$  Hz, H-5), 8.74 (1H, s, H-4), 10.65 (1H, s, H-9);  $^{13}\text{C}$  NMR (100 MHz,  $\text{CDCl}_3$ )  $\delta_{\text{C}}$  87.6 (C-10), 121.1 (C-3, C-6), 122.4 (C-6, C-8), 125.8 (C-4), 127.7 (C-5), 129.7 (C-7), 132.8 (C-8a), 135.6 (C-4a), 163.6 (C-2), and 188.9 (C-9).

**2.2.6. Synthesis of 2-Chloroquinoline-3-carboxylic Acid (8).** Sodium hydroxide solution (1 mL, 10%) was added to a suspension of 2-chloroquinoline-3-carbaldehyde (0.5 g, 0.0026 mol) in water (20 mL). Then a saturated solution of potassium permanganate in water was added dropwise until a definite purple color remains after shaking the solution. The mixture was acidified with 10% sulfuric acid, and a saturated oxalic acid was added to destroy the excess permanganate solution. The carboxylic acid precipitate was isolated by suction filtration. Yield 59.3%; white powder, mp 202–204°C;

$R_f=0.63$  (EtOAc: dichloromethane: methanol = (3:2:3); UV-Vis  $\lambda_{\max}$  (MeOH) 280 nm; IR ( $\text{cm}^{-1}$ , KBr) 3440–2483 (broad band, acid CO<sub>2</sub>-H str), 1725 (C=O str), 1621 (quinoline C=N str.), 1540 and 1496.6 (aromatic C=C str.);  $^1\text{H}$  NMR (400 MHz, DMSO-*d*<sub>6</sub>)  $\delta_{\text{H}}$  7.72 (1H, t,  $J=7.0$  Hz, H-6), 7.92 (1H, t,  $J=7.0$  Hz, H-7), 7.98 (1H, d,  $J=7.8$  Hz, H-8), 8.15 (1H, d,  $J=7.8$  Hz, H-5), 8.93 (1H, s, H-4);  $^{13}\text{C}$  NMR (100 MHz, DMSO-*d*<sub>6</sub>)  $\delta_{\text{C}}$  130.65 (C-3), 131.10 (C-4a), 132.83 (C-8a), 133.21 (C-5), 134.50 (C-6), 137.92 (C-7), 146.93 (C-4), 151.62 (C-8), 152.5 (C-2), and 170.90 (C-9).

**2.2.7. Synthesis of 4-Nitrophenol (10).** Concentrated sulfuric acid (5.5 mL) was added to a 100 mL beaker containing water (7.5 mL). To the solution, finely powdered *p*-nitroaniline (3.5 g, 0.025 mol) and 15 g of finely crushed ice were added and stirred until the *p*-nitroaniline converted into a homogeneous paste. It was cooled to 0–5°C by immersion of the beaker in crushed ice. A cold solution of sodium nitrite (1.8 g) in 4 mL of water was added to it dropwise while keeping temperature below 5°C during the diazotization process. While the diazotization reaction was in progress, a mixture of 16.5 mL concentrated sulfuric acid in 15 mL of water was heated to just boiling in 100 mL round flask, and the diazonium solution was added to it dropwise within 5 minutes. After additional 5 minutes of boiling, the mixture was cooled in ice bath while being stirred continuously. The solid mass was collected by suction filtration and washed with 10 mL of cold water. The crude product was recrystallized in 6M hydrochloric acid. The yield of yellow crystal product was 2.1 g (60%). The melting point was 112–113°C (literature value is 113.8°C). Purity was analyzed with TLC, and its authenticity was ascertained by comparing its melting point with literature value.

**2.2.8. Synthesis of 2-Nitro-12H-chromeno[2,3-*b*]quinolin-12-one (11).** *p*-Nitrophenol (0.34 g, 0.0024 mol), 2-chloro-8-methylquinoline-3-carbaldehyde (0.5 g, 0.0024 mol), potassium carbonate (0.67 g, 0.0047 mol), and moist copper powdered (0.1 g, 0.0016) were added to a 100 mL two-neck round-bottom flask containing N,N-dimethylformamide (20 mL). A water condenser was fitted into one of the necks, and the other one was closed with glass stopper. The mixture was refluxed for 5 hours with the progress followed by TLC. After being cooled to room temperature, it was added to 100 mL crushed ice water. The solid product was separated by suction filtration and washed with 5% sodium hydroxide solution (50 mL). Yield 0.61 g (81.3%); yellow powder, mp 177–179°C;  $R_f=0.67$  (*n*-hexane:EtOAc = 2:1), UV-Vis  $\lambda_{\max}$  (MeOH) 285 nm; IR ( $\text{cm}^{-1}$ , KBr) 3055 (aromatic C-H str.), 1703 (C=O str.), 1615 (quinoline C=N str.), 1577 (aromatic C=C str.), 1512 and 1340 (O=N-O str.);  $^1\text{H}$  NMR: (400 MHz,  $\text{CDCl}_3$ )  $\delta_{\text{H}}$  6.97 (2H, t,  $J=7.4$  Hz, H-8, H-9), 7.04 (2H, d,  $J=8.4$  Hz, H-4, H-7), 7.55 (2H, t,  $J=7.4$  Hz, H-1, H-10), 7.96 (2H, d,  $J=8.0$  Hz, H-3, H-11);  $^{13}\text{C}$  NMR (100 MHz,  $\text{CDCl}_3$ )  $\delta_{\text{C}}$  111.4

(C-11a, C-12a), 117.8 (C-1, C-4, C-9), 119.6 (C-7, C-10, C-10a), 131.0 (C-3, C-8), 137.0 (C-2, C-6a, C-11), 162.2 (C-4a, C-5a), 175.0 (C-12).

**2.2.9. Synthesis of 2-Methylacetanilide (13).** To a 250 mL round-bottom flask, *o*-toluidine (22 mL, 22.2 g, 0.207 mol), acetic anhydride (23 mL, 24.84 g, 0.24 mol), acetic acid (23 mL, 24.15 g, 0.40 mol), and zinc powder (0.2 g, 0.003 mol) were added. The mixture was refluxed for an hour using water condenser. It was cooled to room temperature and added to 200 mL crushed ice water. The product was collected by suction filtration. Yield 21.2 g (69%); white powder; mp 108–110°C (Lit. 109–112°C).

**2.2.10. Synthesis of 2-Chloro-8-methylquinoline-3-carbaldehyde (14).** To a 100 mL round-bottom flask equipped with drying tube, *N,N*-dimethylformamide (20 mL, 18.88 g, 0.26 mol) was added, and the mixture was cooled to 0°C using ice bath. Then phosphorus oxychloride (70 mL, 115.15 g, 0.75 mol) was added dropwise from dropping funnel guarded by drying tube which was fitted to flask with adaptor while being stirred by magnetic stirrer for 30 minutes. Next, *N*-(*o*-tolyl)acetamide (13.5 g, 0.1 mol) was added to it, the dropper funnel was replaced by air condenser with guarding tube, and the mixture was heated for 22 hours on oil bath at 85–90°C. After that, it was cooled to room temperature and poured into a beaker containing 400 mL crushed ice water, while being stirred with glass rod. The yellow solid product was collected by suction filtration and washed with cold water. The crude yield was 9.2 g (44.77%), and it was recrystallized in ethyl acetate. The final pure product was 6.8 g (33.09%); pale yellow crystal; mp 136–140°C;  $R_f = 0.30$  (n-hexane:EtOAc = 9:1), UV-Vis  $\lambda_{max}$  (MeOH) 295 nm; IR (cm<sup>-1</sup>, KBr) 3223, 3025 (arom-C-H.), 2956 (alip-C-H), 2837 (alip-C-H), 1683.3 (C=O str.), 1621 (quinoline C=N str.), 1579 (aromatic C=C str.); <sup>1</sup>H NMR (400 MHz; CDCl<sub>3</sub>)  $\delta_H$  2.80 (3H, s, H-10), 7.53 (1H, t, H-6), 7.70 (1H, d, H-7), 7.78 (1H, d, H-5), 8.70 (1H, s, H-4), 10.6 (1H, s, H-9); <sup>13</sup>C NMR (100 MHz, CDCl<sub>3</sub>)  $\delta_C$  17.8 (C-10), 126.0 (C-3), 126.5 (C-6), 127.5 (C-5), 127.8 (C-4a), 133.6 (C-7), 136.9 (C-8), 140.4 (C-4), 148.7 (C-2), 149.4 (C-8a) and 189.5 (C-1).

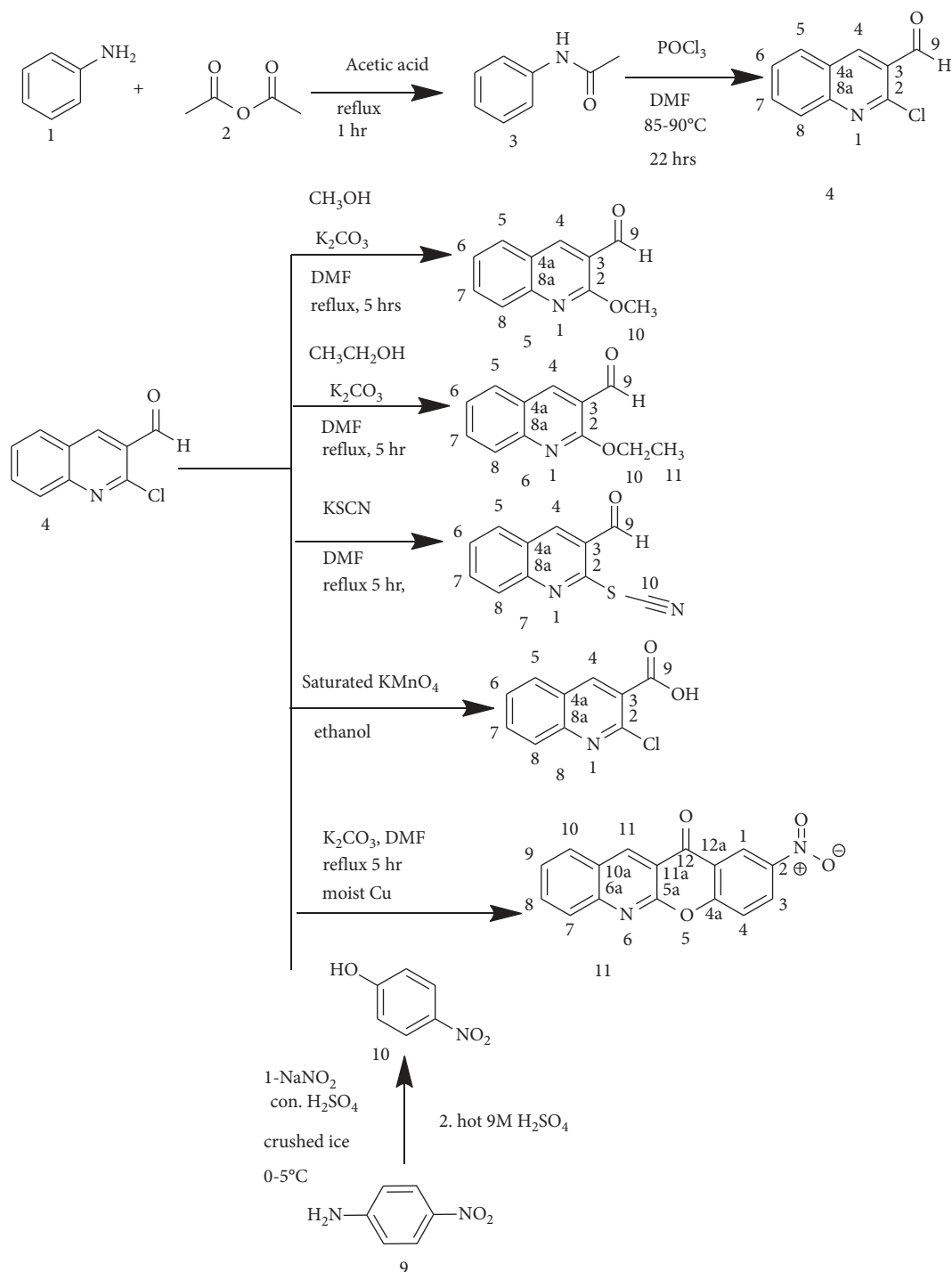
**2.2.11. Synthesis of 8-Methyl-2-oxoquinoline-3-carbaldehyde (15).** 2-Chloro-8-methylquinoline-3-carbaldehyde (0.5 g, 0.0024 mol) was added to a mixture of 6M HCl (10 mL) and glacial acetic acid (10 mL). The mixture was refluxed for 3 hours, at which the TLC analysis showed complete disappearance of the starting material. Then the acetic acid mixture was removed with distillation under reduced pressure. The solid residue was washed with cold water and allowed to dry in wood cupboard. The amount of the product was 395 mg. Yield 86.5%; yellow powder; mp 176–178°C;  $R_f = 0.41$  (n-hexane:EtOAc = 1:1); UV-Vis  $\lambda_{max}$  (MeOH) 375 nm; IR (cm<sup>-1</sup>, KBr) 3429 (O-H str.), 3179.5 (NH str.), 3023 (aromatic C-H), 2919.8 (aliphatic CH-str.), 2837.2 (aliphatic C-H) 1673 (C=O str.), 1610 (quinoline

C=N str.), 1558 and 1465 (aromatic C=C str.); <sup>1</sup>H NMR (400 MHz; CDCl<sub>3</sub>)  $\delta_H$  2.56 (3H, s, C-10), 7.23 (1H, t,  $J = 7.5$  Hz, H-6), 7.51 (1H, d,  $J = 7.32$  Hz, H-7) 7.61 (1H, m,  $J = 7.7$  Hz, H-5), 8.49 (1H, s, H-4) and 10.48 (1H, s, H-9); <sup>13</sup>C NMR (100 MHz, CDCl<sub>3</sub>)  $\delta_C$  16.7 (C-10), 117.9 (C-6), 123.3 (C-3, C-8), 129.1 (C-4a, C-7), 135.0 (C-5), 139.1 (C-8a), 144.2 (C-4), 162.7 (C-2), 190.00 (C-9).

**2.2.12. Synthesis of (2-Methoxy-8-methylquinolin-3-yl)methanol (16).** A gram of sodium (0.043 mol) was dissolved in 10 mL methanol, and 2-chloro-8-methylquinoline-3-carbaldehyde (0.5 g, 0.0024 mol) and 10 mL of *N,N*-dimethylformamide were added to it. The mixture was refluxed for 6 hours, at which TLC analysis showed complete disappearance of the aldehyde. After removal of methanol using distillation, the remaining content was cooled to room temperature and added to 100 mL ice-cold water. The precipitate was collected by fractional distillation. Yield 53%; gray powder, mp 98–99°C;  $R_f = 0.51$  (n-hexane:EtOAc = 3:1), UV-Vis  $\lambda_{max}$  (MeOH) 315 nm; IR (cm<sup>-1</sup>, KBr): 3470 (br-alcohol CHO-H str.), 3013 (aromatic C-H str.), 2930.9 (aliphatic C-H str.), 1625 (quinoline C=N str.), 1589.6 and 1475.5 (aromatic C=C str.); <sup>1</sup>H NMR (400 MHz; CDCl<sub>3</sub>)  $\delta_H$  2.80 (3H, s, H-10), 4.11 (3H, s, H-9), 4.79 (2H, s, H-1), 7.28 (1H, t,  $J = 7.58$  Hz, H-6), 7.42 (1H, d,  $J = 7.0$  Hz, H-7), 7.58 (2H, d,  $J = 8.34$  Hz, H-5), 7.86 (1H, s, H-4); <sup>13</sup>C NMR (100 MHz, CDCl<sub>3</sub>)  $\delta_C$  18.1 (C-10), 51.3 (C-9), 61.9 (C-1), 123.8 (C-3), 124.1 (C-6), 124.2 (C-4a), 125.0 (C-5), 129.4 (C-7), 135.1 (C-8), 135.9 (C-4), 144.7 (C-8a), 160.2 (C-2).

**2.2.13. Synthesis of (2-Ethoxy-8-methylquinolin-3-yl)methanol (17).** Sodium (1 g, 0.043 mol) was dissolved in ethanol (10 mL), and 0.5 g (0.0024 mol) of 2-chloroquinoline-3-carbaldehyde and 10 mL of *N,N*-dimethylformamide were added to it. The mixture was refluxed for 5 hours, at which TLC analysis showed complete disappearance of the aldehyde. The ethanol was removed by distillation, and the remaining content was cooled to room temperature and added to 100 mL cold water. The precipitate was collected by fractional distillation. Yield 82.7%; dull brown; mp 85–87°C;  $R_f = 0.54$  (n-hexane:EtOAc = 3:1); UV-Vis  $\lambda_{max}$  (MeOH) 315 nm; IR (cm<sup>-1</sup>, KBr) 3502–3148 (OH str.), 3025 (aromatic C-H str.), 2930.9 (aliphatic C-H str.), 1625 (quinoline C=N str.), 1582 (aromatic C=C str.); <sup>1</sup>H NMR (400 MHz; CDCl<sub>3</sub>)  $\delta_H$  1.5 (3H, t,  $J = 7.01$  Hz, H-10), 2.74 (3H, s, H-11) 4.63 (2H, q,  $J = 7.01$  Hz, H-9), 4.48 (2H, s, H-1), 7.26 (1H, t,  $J = 7.04$  Hz, H-6), 7.47 (1H, d,  $J = 6.89$  Hz, H-7), 7.56 (1H, d,  $J = 7.80$  Hz, H-5), 7.93 (1H, s, H-4); <sup>13</sup>C NMR (100 MHz, CDCl<sub>3</sub>)  $\delta_C$  13.7 (C-10), 19.3 (C-11), 61.5 (C-1), 61.8 (C-9), 123.0 (C-9), 124.2 (C-6), 124.90 (C-4a), 125.0 (C-5), 130.3 (C-7), 135.0 (C-8), 135.8 (C-4), 144.7 (C-8a), 158.3 (C-2).

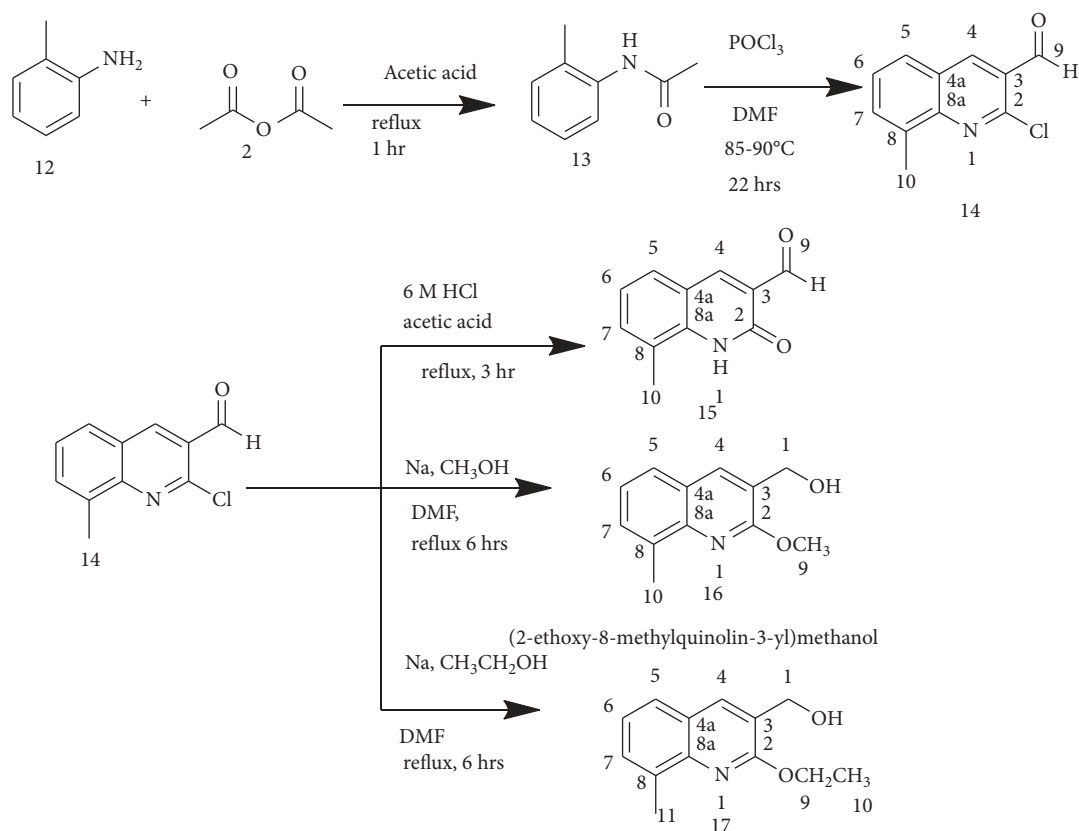
**2.3. Antibacterial Activity.** Antibacterial activities of the synthesized compounds were tested using the paper disc-diffusion method. In the process, two Gram-positive bacteria (*Bacillus subtilis* ATCC6633 and *Staphylococcus aureus* ATCC25923) and two Gram-negative bacteria



SCHEME 1: Synthesis of 2-chloroquinoline-3-carbaldehyde and its derivatives.

(*Escherichia coli* ATCC 25922 and *Pseudomonas aeruginosa* ATCC 27853) were used to evaluate the antibacterial activities. The medium was prepared from molten nutrient and Müller–Hinton agar. Ciprofloxacin was the standard drug used as positive control while DMSO was used as negative control. The four bacterial strains were tested with 300 and 500  $\mu\text{g}/\text{mL}$  concentration using paper disc-diffusion method. Each of the ten compounds was dissolved in DMSO at concentrations of 300 and 500  $\mu\text{g}/\text{mL}$

mL, 6 mm diameter Whatman filter paper discs were soaked with 1 mL solution of the above two concentrations for each compound, and then these saturated paper discs were inoculated at the center of each Petri dish having bacterial lawn in triplicate. The plates were incubated at 37 $^\circ\text{C}$  for 48 h, and the inhibition zone that appeared around the paper disc in each plate was determined by measuring the diameter of the inhibition zone.



SCHEME 2: Synthesis of 2-chloro-8-methylquinoline-3-carbaldehyde and its derivatives.

#### 2.4. Radical Scavenging Activity of the Synthesized Compounds.

The radical scavenging activity of the synthesized compounds was evaluated with 1,1-diphenyl-2-picrylhydrazyl (DPPH). In the process, 0.04 mg/mL solution of DPPH in methanol was prepared; 1 mL of this solution was poured into 4 mL of the synthesized samples in methanol to furnish four different concentrations (12.5, 25, 50, 100  $\mu\text{g}/\text{mL}$ ); and control was made by adding 1 mL of the DPPH solution to 4 mL of methanol, while 4 mL methanol was used as a blank. The mixtures were shaken and allowed to stand at 37°C for 30 min in dark oven, and absorbance was recorded at 517 nm using double beam UV-Vis spectrophotometer. Ascorbic acid was used for reference standard in similar concentration as above. Percentage inhibition of DPPH radical was determined using the following equation:

$$\% \text{ inhibition} = \frac{A_0 - A_1}{A_0} \times 100, \quad (1)$$

where  $A_0$  is the absorbance of control reaction and  $A_1$  is the absorbance in presence of test or standard sample [21].

**2.5. Molecular Docking Analysis of the Synthesized Compounds.** AutoDock Vina with standard protocol was used to dock the proteins (PDB ID: 6F86; PDB ID: 2XCT) and synthesized compounds (4–17) into the active site of proteins [22]. The chemical structures of compounds 4–17

were drawn using ChemOffice tool (ChemDraw 16.0) assigned with proper 2D orientation, and energy of each molecule was minimized using ChemBio3D. The energy-minimized ligand molecules were then used as input for AutoDock Vina, in order to carry out the docking simulation [22]. The crystal structures of receptor molecule *E. coli* gyrase B (PDB ID: 6F86) and *S. aureus* gyrase complex with ciprofloxacin and DNA (PDB ID: 2XCT) were downloaded from protein data bank. The protein preparation was done using the reported standard protocol [23] by removing the cocrystallized ligand, selected water molecules, and cofactors; the target protein file was prepared by leaving the associated residue with protein using Auto Preparation of target protein file AutoDock 4.2 (MGLTools 1.5.6). The graphical user interface program was used to set the grid box for docking simulations. The grid was set so that it surrounds the region of interest in the macromolecule. The docking algorithm provided with AutoDock Vina was used to search for the best docked conformation between ligand and protein [22–24]. During the docking process, a maximum of nine conformers were considered for each ligand. The conformations with the most favorable (least) free binding energy were selected for analyzing the interactions between the target receptor and ligands by Discovery Studio Visualizer and PyMOL. The ligands are represented in different color; H-bonds and the interacting residues are represented in ball and stick model representation.

TABLE 1: The inhibition zone of the synthetic compound in mm (mean  $\pm$  SD).

Bacterial strains	Conc. ( $\mu$ g/mL)	Compounds														
		4	5	6	7	8	11	14	15	16	17	Ciprofloxacin				
<i>E. coli</i>	300	6.33 $\pm$ 0.44	NA	NA	NA	NA	9.00 $\pm$ 0.55	7.33 $\pm$ 0.66	NA	NA	NA	8.00 $\pm$ 0.67	NA	19.0 $\pm$ 0.67		
	500	6.67 $\pm$ 0.89	NA	NA	NA	NA	11.33 $\pm$ 1.11	11.0 $\pm$ 1.33	NA	NA	NA	9.33 $\pm$ 0.89	NA	21.0 $\pm$ 0.55		
<i>B. subtilis</i>	300	7.0 $\pm$ 0.67	NA	7.0 $\pm$ 0.67	7.00 $\pm$ 0.67	6.67 $\pm$ 0.89	6.67 $\pm$ 0.89	NA	6.67 $\pm$ 0.44	NA	NA	6.33 $\pm$ 0.44	6.33 $\pm$ 0.44	30.0 $\pm$ 0.67		
	500	7.67 $\pm$ 0.44	NA	7.67 $\pm$ 0.44	7.33 $\pm$ 0.44	7.00 $\pm$ 0.67	7.00 $\pm$ 0.67	NA	7.33 $\pm$ 0.44	NA	NA	7.33 $\pm$ 0.44	7.33 $\pm$ 0.44	33.0 $\pm$ 0.67		
<i>S. aureus</i>	300	6.33 $\pm$ 0.44	6.00 $\pm$ 0.00	NA	NA	6.00 $\pm$ 0.00	6.00 $\pm$ 0.00	NA	NA	NA	6.00 $\pm$ 0.44	NA	NA	9.0 $\pm$ 0.67		
	500	7.0 $\pm$ 0.67	6.33 $\pm$ 0.44	6.00 $\pm$ 0.00	NA	6.33 $\pm$ 0.44	6.33 $\pm$ 0.44	NA	NA	NA	6.67 $\pm$ 0.44	NA	NA	11.0 $\pm$ 0.67		
<i>P. aeruginosa</i>	300	7.0 $\pm$ 0.67	7.67 $\pm$ 0.44	8.0 $\pm$ 0.67	6.33 $\pm$ 0.44	7.00 $\pm$ 0.00	7.00 $\pm$ 0.00	6.00 $\pm$ 0.00	6.33 $\pm$ 0.44	8.33 $\pm$ 0.44	8.33 $\pm$ 0.44	NA	NA	7.00 $\pm$ 0.00		
	500	9.0 $\pm$ 0.67	9.33 $\pm$ 0.44	9.67 $\pm$ 1.11	6.33 $\pm$ 0.44	8.00 $\pm$ 0.67	8.00 $\pm$ 0.67	6.33 $\pm$ 0.44	7.33 $\pm$ 0.44	10.0 $\pm$ 0.44	10.0 $\pm$ 0.44	NA	NA	8.33 $\pm$ 0.44		

NA: no inhibition zone; results are expressed as M $\pm$ SD of triplicates.

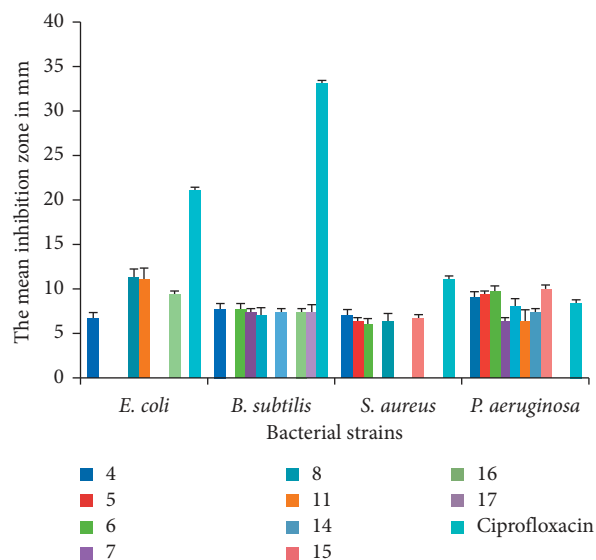


FIGURE 1: The inhibition zone of the synthetic compounds in mm (mean  $\pm$  SD) at 500  $\mu\text{g/mL}$ .

### 3. Results and Discussion

**3.1. Chemistry.** In an attempt to generate quinoline derivatives which have antibacterial properties, various quinoline derivatives were prepared using various reaction conditions. In the process, N-(o-tolyl)acetamide and acetanilide were prepared by refluxing the corresponding aniline in acetic acid and acetic anhydride mixtures. Then 2-chloroquinoline-3-carbaldehyde and 2-chloro-8-methylquinoline-3-carbaldehyde were prepared from the acetanilide by the Vilsmeier approach. The chlorine in position 2 of quinolines was substituted by various nucleophiles by refluxing 2-chloroquinoline-3-carbaldehyde and 2-chloro-8-methylquinoline-3-carbaldehyde in N,N-dimethylformamide with various nucleophilic reagents in basic medium. Potassium carbonate was used to induce the basic medium. Refluxing 2-chloro-8-methylquinoline-3-carbaldehyde in 6M HCl and acetic acid (1:1) mixture afforded 8-methyl-2-oxoquinoline-3-carbaldehyde. The carbaldehyde functional group of quinoline was oxidized to carboxylic acid by permanganate method and was subsequently reduced to alcohol using metallic sodium. The overall sequence of reactions used in the synthesis of various targeted quinoline derivatives are illustrated in Schemes 1 and 2.

The structure elucidation of the synthesized compounds was accomplished using UV-Vis, FTIR, and NMR spectroscopic methods.

**3.2. Antibacterial Activity.** Quinolines are pharmacologically active compounds used to treat various life threatening diseases. In an attempt to find out lead compounds against bacteria, a series of quinoline derivatives have been synthesized and subsequently evaluated for their antibacterial activities against various strains of bacterial pathogens. The results obtained are depicted in Table 1 and Figure 1.

The above data shows all synthesized compounds displayed medium to good activity against two or more bacterial strains. The mean inhibition zones ranged from the lowest (6 mm at 300  $\mu\text{g/mL}$ ) to the highest (11.3 mm at 500  $\mu\text{g/mL}$ ). Three of the ten compounds, 8, 11, and 16, showed good activities against *Escherichia coli*, among which 11 and 8 revealed better activities with mean inhibition zone of  $11.00 \pm 1.33$  and  $11.33 \pm 1.11$  mm diameter at 500  $\mu\text{g/mL}$ , respectively. Seven of the ten compounds (4, 6, 8, 7, 14, 16, and 17) (Figure 1) showed antibacterial activity against *Bacillus subtilis*, but maximum inhibition zone ( $7.67 \pm 0.44$  mm) was observed in compounds 4 and 6. None of the synthetic compounds demonstrated activity against *Staphylococcus aureus* except 4, 5, 8, and 15 which showed slight activity. Among the synthetic compounds, 4, 5, 6, and 15 displayed moderate activity against *Pseudomonas aeruginosa*, and the maximum inhibition zone was  $10.00 \pm 0.44$  mm for compound 15 but only  $8.33 \pm 0.44$  mm for ciprofloxacin at the same concentration (500  $\mu\text{g/mL}$ ). Compounds 4 and 8 displayed moderate to good activity against all tested bacterial species, while compound 17 showed no activity against all tested organisms except *Bacillus subtilis* with inhibition zones of  $6.33 \pm 0.44$  mm and  $7.33 \pm 0.44$  mm at concentrations of 300 and 500  $\mu\text{g/mL}$ , respectively.

**3.3. Radical Scavenging Activity of the Synthetic Compounds.** DPPH assay was widely used to assess the ability of compounds as scavengers of free radicals and hence evaluate the antioxidant activity of synthetics compounds or phytochemicals. Compounds exhibiting antioxidant activity reduced the absorbance at 517 nm, which is due to DPPH radical in addition to their ability to turn the purple colored DPPH to yellow. In this work, the radical scavenging activity of the synthesized compounds was evaluated using DPPH, and the findings are depicted in Table 2.



TABLE 2: Percent radical scavenging activity of the synthesized compounds.

Conc. ( $\mu\text{g/mL}$ )	Compounds											Ascorbic acid
	4	5	6	7	8	11	14	15	16	17	17	
<b>12.5</b>	20.9 $\pm$ 0.44	14.7 $\pm$ 0.89	16.7 $\pm$ 0.33	37.4 $\pm$ 0.44	22.8 $\pm$ 0.71	18.1 $\pm$ 0.44	5.8 $\pm$ 0.71	1.9 $\pm$ 0.33	16.7 $\pm$ 0.67	18.3 $\pm$ 0.33	18.3 $\pm$ 0.33	83.2 $\pm$ 0.44
<b>25.0</b>	22.8 $\pm$ 0.67	18.9 $\pm$ 0.44	16.9 $\pm$ 0.67	45.2 $\pm$ 0.67	24.8 $\pm$ 0.44	21.7 $\pm$ 0.44	6.6 $\pm$ 0.67	12.2 $\pm$ 0.67	20.6 $\pm$ 0.0	23.9 $\pm$ 0.33	23.9 $\pm$ 0.33	84.9 $\pm$ 0.67
<b>50.0</b>	26.7 $\pm$ 0.55	26.1 $\pm$ 0.67	23.7 $\pm$ 0.71	51.9 $\pm$ 0.67	28.7 $\pm$ 0.67	23.7 $\pm$ 0.55	9.4 $\pm$ 0.55	22.8 $\pm$ 0.55	25.9 $\pm$ 0.71	24.5 $\pm$ 0.44	24.5 $\pm$ 0.44	85.1 $\pm$ 0.0
<b>100.0</b>	32.64 $\pm$ 0.71	31.5 $\pm$ 0.89	35.4 $\pm$ 0.44	67.0 $\pm$ 0.55	33.7 $\pm$ 0.67	23.9 $\pm$ 0.67	15.0 $\pm$ 0.55	23.4 $\pm$ 0.67	33.2 $\pm$ 0.55	25.1 $\pm$ 0.67	25.1 $\pm$ 0.67	85.4 $\pm$ 0.71

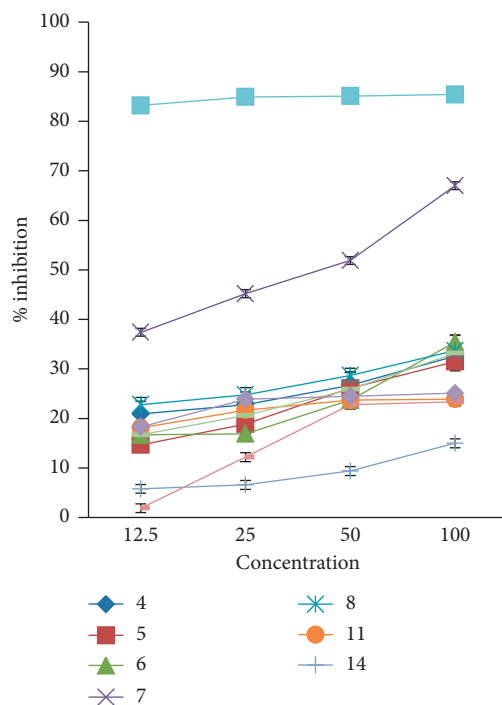


FIGURE 2: Percentage inhibition of DPPH radical by the synthetic compounds.

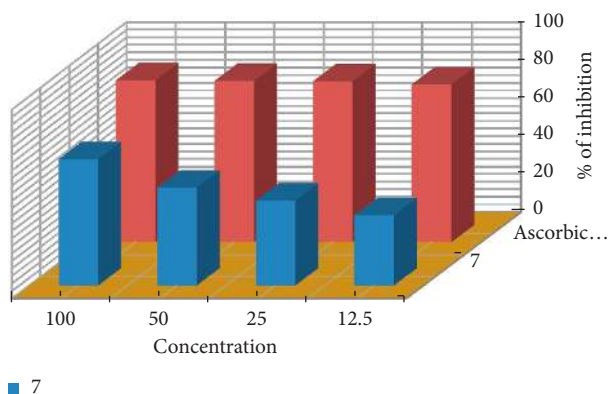
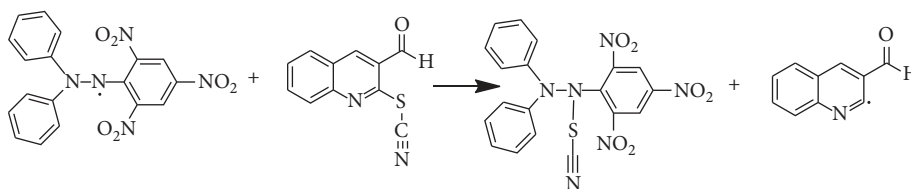


FIGURE 3: Comparison of % inhibition of compound 7 with ascorbic acid.



SCHEME 3: Proposed mechanism of action of compound 7.

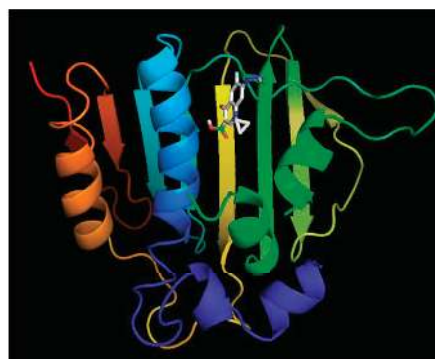
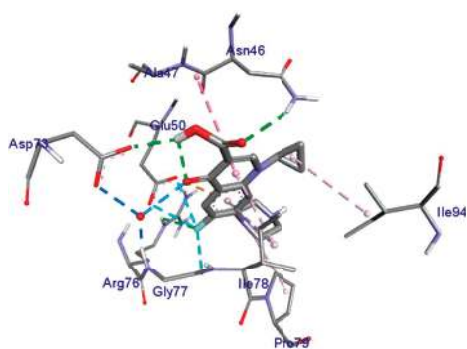
The DPPH radical scavenging activity of the synthesized compounds was compared with ascorbic acid which is used as positive control, and the result is presented in Figure 2.

Compound 7, which displayed better radical scavenging activity in the present work, has been elaborated in comparison with ascorbic acid using 3D diagram (Figure 3).

The data in Table 2 and Figure 2 reveal that nine of the synthetic compounds showed moderate antioxidant activities, while compound 7 (Figure 3) exhibited better antioxidant activity (67% radical scavenging activity at 100  $\mu\text{g}/\text{mL}$  concentration) among them all. 1,1-Diphenyl-2-picrylhydrazyl (DPPH) is a stable free radical accepting hydrogen

TABLE 3: Molecular docking value of compounds 4–17 against *E. coli* DNA gyrase B.

Compounds	Affinity (kcal/mol)	H-bond	Receptor interactions
4	-6.2	Asp-73	Val-43, Val-71, Ile-78, Ala-47
5	-6.2	Asp-73, Thr-165, Gly-77	Ile-94, Ile-78
6	-6.4	Gly-77, Thr-165	Asp-73, Ile-94, Ile-78, Ala-47
7	-6.3	Asn-46, Thr-165, Gly-77	Asp-73, Val-43, Val-167, Ala-47
8	-6.3	Asn-46	Asp-73, Arg-76, Ala-47, Glu-50, Gly-77, Ile-78, Pro-79, Gly-75, Thr-165
11	-7.3	Arg-76, Asn-46, Gly-77, Thr-165	Asp-73, Ile-78, Ile-94, Pro-79, Glu-50, Gly-75
14	-6.3	-	Ile-78, Val-167, Val-120
15	-6.2	-	Ala-47, Asn-46, Ile-78, Thr-165, Val-167
16	-6.0	Asp-73	Ile-78
17	-6.3	Asp-73, Gly-77	Ala-47, Glu-50, Ile-78, Pro-79, Thr-165
Ciprofloxacin	-6.9	Asp-73, Arg-76, Asn-46	Ala-47, Ile-78, Ile-94, Pro-79, Glu-50, Gly-77

FIGURE 4: The binding interactions of ciprofloxacin against *E. coli* DNA gyrase B (PDB ID: 6F86).

from a corresponding donor, which causes it to lose the characteristic deep purple ( $\lambda_{\max}$  517 nm) color. In compound 7, there is no such easily transferable hydrogen; however, sulfur of thiocyanate functional group may donate an electron to lone pair electron on the nitrogen atom to form bond with sulfur (Scheme 3).

**3.4. In Silico Molecular Docking Evaluation.** In general, antimicrobial agents target the key components of bacterial metabolism to disable the bacteria such as cell-walls, DNA gyrase, DNA-directed RNA polymerase, protein synthesis, and enzymes. DNA gyrase, an enzyme belonging to a member of bacterial topoisomerase, controls the topology of DNA during transcription, replication, and recombination by introducing transient breaks to both DNA strands [25–27]. In this regard, bacterial DNA gyrase is essential for bacterial survival and therefore necessary to be exploited as an antibacterial drug target [28]. Therefore, in the present study, the molecular docking analysis of the synthesized compounds was carried out to investigate their binding pattern with DNA gyrase and compare them with standard inhibitor (ciprofloxacin). The synthesized compounds (4–17) were found to have minimum binding energy ranging from -6.2 to -7.3 kcal/mol (Table 3), with the best result achieved using compound 11 (-7.3 kcal/mol). The binding affinity, H-bond, and residual interaction of ten

compounds and ciprofloxacin were summarized in Table 3. Compared to ciprofloxacin, the synthesized compounds (4–17) showed similar residual interactions profile with amino acid residues Ile-94, Pro-79, Glu-50, Gly-77, Ile-78, and Ala-47 and H-bond with Asp-73, Arg-76, and Asn-46. Compounds 5, 6, and 7 have additional hydrogen bonding interaction with amino acid residue Thr-165. The compounds 4 (Val-43, Val-71), 7 (Val-167), 14 (Val-120 and Val-167), and 15 (Val-167) have shown additional hydrophobic interaction with amino acid residues. The residual amino acid interactions of synthesized ligands (except 14 and 15) with DNA gyrase (6f86) in this study were well in agreement with the previously reported binding modes that include the crucial interactions between the ligand, Asp-73, and the water molecule [23]. The *in silico* interaction results match the *in vitro* analysis of the synthesized compounds; 4 (-6.2 kcal/mol), 11 (-7.3 kcal/mol), 8 (-6.3 kcal/mol), and 16 (-6.0 kcal/mol) showed good activities against *E. coli*, among which compounds 8 (-6.3 kcal/mol) and 11 (-7.3 kcal/mol) revealed better activity. The compounds 14 and 15 docking results partially matched the ciprofloxacin interactions with amino acid residues. Based on the *in silico* molecular docking analysis results, compounds 8 and 11 showed comparable residual interactions and docking score of ciprofloxacin. Therefore, compound 11 might have the best antibacterial agents among the compounds reported herein. The binding

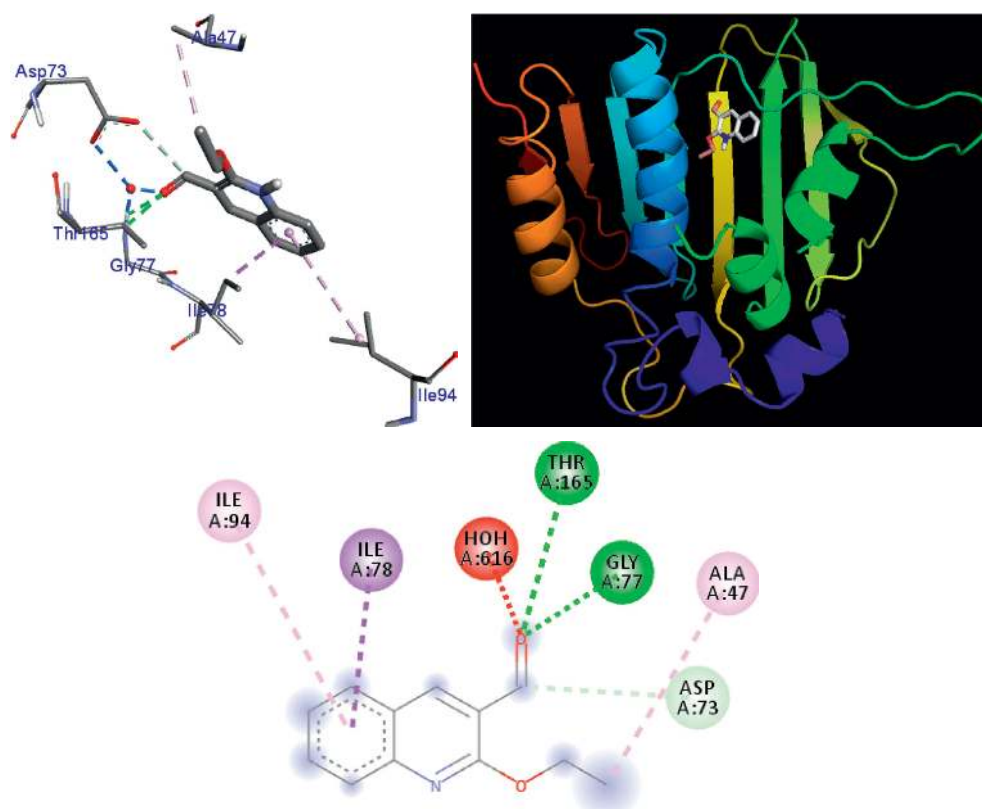


FIGURE 5: The binding interactions of compound **6** against *E. coli* DNA gyrase B (PDB ID: 6F86).

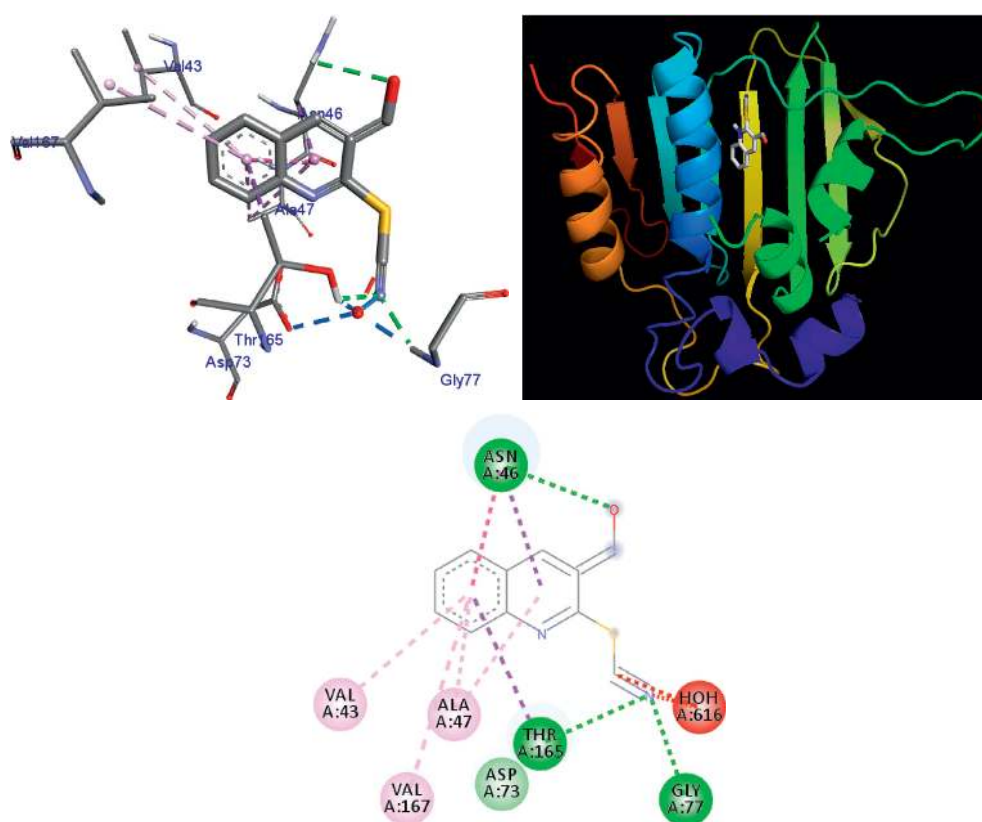


FIGURE 6: The binding interactions of compound **7** against *E. coli* DNA gyrase B (PDB ID: 6F86).

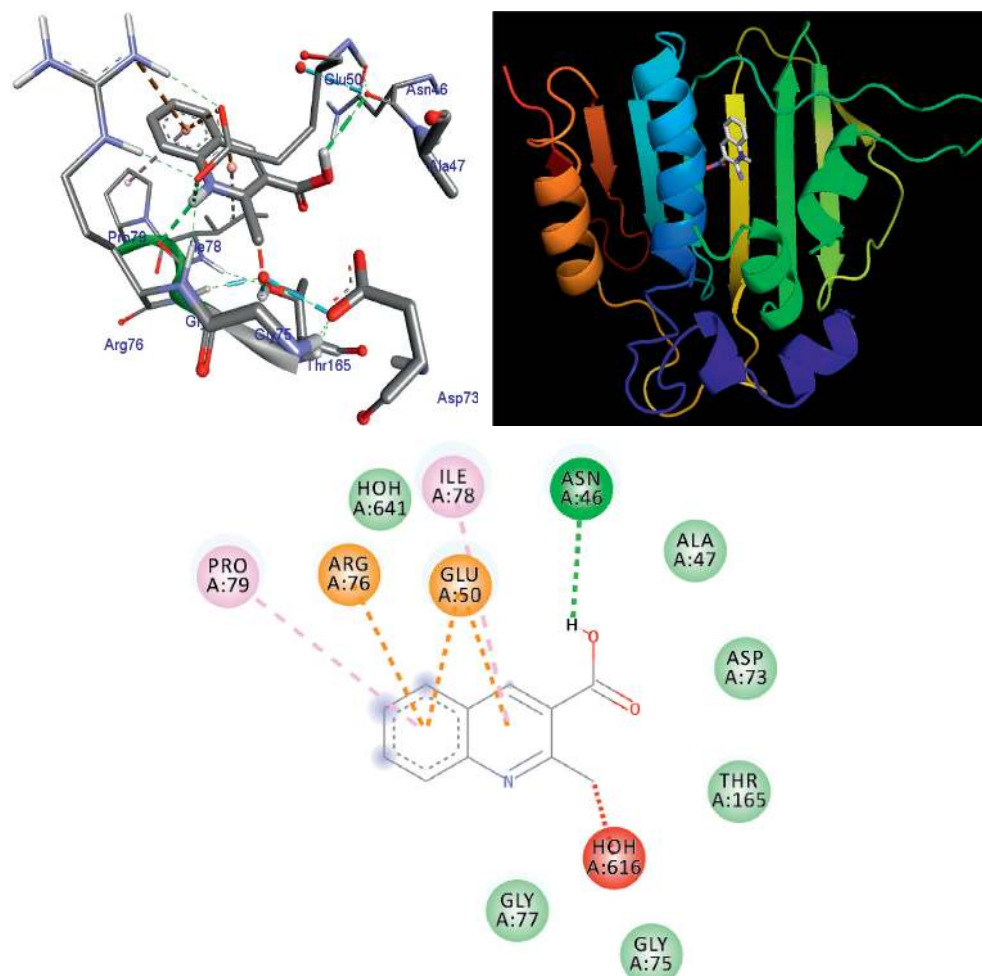


FIGURE 7: The binding interactions of compound 8 against *E. coli* DNA gyrase B (PDB ID: 6F86).

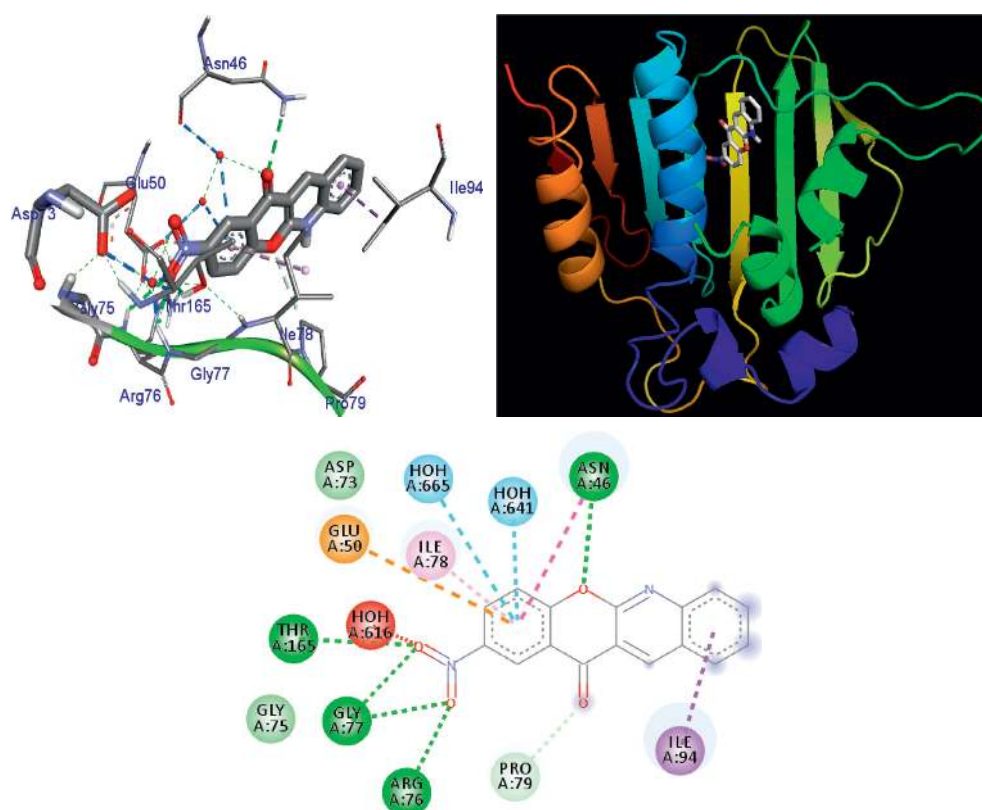


FIGURE 8: The binding interactions of compound 11 against *E. coli* DNA gyrase B (PDB ID: 6F86).

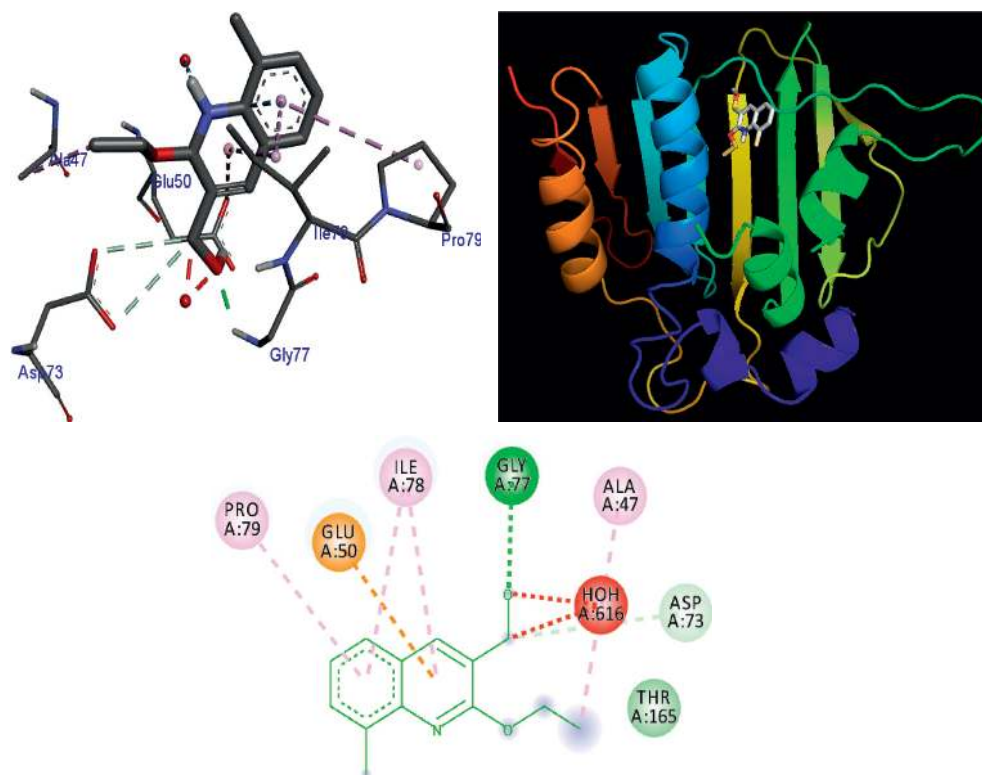


FIGURE 9: The binding interactions of compound 17 against *E. coli* DNA gyrase B (PDB ID: 6F86).

affinity, H-bond, and residual interaction of ten compounds were summarized in Table 3.

The 3-dimensional binding interaction of compounds 6, 7, 8, 11, 17 and ciprofloxacin against *E. coli* gyrase B complex is illustrated in Figures 4–9. The docking results of compounds 4, 5, 14, 15, and 16 against *E. coli* gyrase B complex and compounds 4–17 against *S. aureus* gyrase B complex are given as supplementary data.

#### 4. Conclusion

The quinoline heterocycle is a useful scaffold to develop bioactive molecules. In the present work, we synthesized series of quinolin derivatives by application of Vilsmeier–Haack reaction. Various nucleophiles were introduced into 2-chloroquinoline-3-carbaldehyde and 2-chloro-8-methylquinoline-3-carbaldehyde by substitution of chlorine using different reaction conditions. The carbaldehyde functional group was further manipulated to carboxylic acid using potassium permanganate method and reduced to alcohols with metallic sodium. All synthesized compounds were characterized by TLC, melting point,  $^1\text{H}$  NMR,  $^{13}\text{C}$  NMR, and UV-Vis spectroscopy. The antibacterial activities of the synthesized compounds were screened by the disc-diffusion method against two Gram-negative and two Gram-positive bacteria, and most of them were found to have moderate activities against the bacterial strains used for the screening. Among them, compounds 6 and 15 exhibited maximum activity against *Pseudomonas aeruginosa* compared to the standard drug ciprofloxacin. The *in silico* molecular docking

study of the synthesized compounds was performed to assess the binding mode of these compounds against DNA gyrase B (PDB ID: 6F86), and the result was in good harmony with antibacterial assay result. Generally, the synthesized compounds have potential of antibacterial activity and can be further optimized to serve as lead compounds.

#### Data Availability

The data used to support the findings of this study are included within the manuscript and also submitted as Supplementary Materials.

#### Conflicts of Interest

The authors assert that there are no conflicts of interest regarding the publication of this paper.

#### Acknowledgments

The authors are thankful to Adama Science and Technology University for funding this research.

#### Supplementary Materials

The  $^1\text{H}$  NMR and  $^{13}\text{C}$  NMR spectra of the synthesized compounds. Figure 1:  $^1\text{H}$  NMR (400 MHz,  $\text{CDCl}_3$ ) spectrum of 2-chloroquinoline-3-carbaldehyde (4). Figure 2:  $^{13}\text{C}$  NMR (100 MHz,  $\text{CDCl}_3$ ) spectrum of 2-chloroquinoline-3-carbaldehyde (4). Figure 3:  $^1\text{H}$  NMR (400 MHz,  $\text{CDCl}_3$ ) spectrum of 2-methoxyquinoline-3-carbaldehyde (5).

Figure 4:  $^{13}\text{C}$  NMR (100 MHz,  $\text{CDCl}_3$ ) spectrum of 2-methoxyquinoline-3-carbaldehyde (5). Figure 5:  $^1\text{H}$  NMR (400 MHz,  $\text{CDCl}_3$ ) spectrum of 2-ethoxyquinoline-3-carbaldehyde (6). Figure 6:  $^{13}\text{C}$  NMR (100 MHz,  $\text{CDCl}_3$ ) spectrum of 2-ethoxyquinoline-3-carbaldehyde (6). Figure 7:  $^1\text{H}$  NMR (400 MHz,  $\text{DMSO-d}_6$ ) spectrum of 2-thiocyanatoquinoline-3-carbaldehyde. Figure 8:  $^1\text{H}$  NMR (400 MHz,  $\text{DMSO-d}_6$ ) spectrum of 2-chloroquinoline-3-carboxylic acid (8). Figure 9:  $^{13}\text{C}$  NMR (100 MHz,  $\text{DMSO-d}_6$ ) spectrum of 2-ethoxyquinoline-3-carbaldehyde (8). Figure 10:  $^1\text{H}$  NMR (400 MHz,  $\text{CDCl}_3$ ) spectrum of 2-nitro-12H-chromeno[2,3-b]quinolin-12-one (11). Figure 11:  $^{13}\text{C}$  NMR (100 MHz,  $\text{CDCl}_3$ ) spectrum of 2-nitro-12H-chromeno[2,3-b]quinolin-12-one (11). Figure 12:  $^1\text{H}$  NMR (400 MHz;  $\text{CDCl}_3$ ) spectrum of 2-chloro-8-methylquinoline-3-carbaldehyde (14). Figure 13:  $^{13}\text{C}$  NMR (100 MHz;  $\text{CDCl}_3$ ) spectrum of 2-chloro-8-methylquinoline-3-carbaldehyde (14). Figure 14:  $^1\text{H}$  NMR (400 MHz;  $\text{CDCl}_3$ ) spectrum of 8-methyl-2-oxoquinoline-3-carbaldehyde (15). Figure 15:  $^{13}\text{C}$  NMR (100 MHz;  $\text{CDCl}_3$ ) spectrum of 8-methyl-2-oxoquinoline-3-carbaldehyde (15). Figure 16:  $^1\text{H}$  NMR spectrum (400 MHz;  $\text{CDCl}_3$ ) of (2-methoxy-8-methylquinolin-3-yl)methanol (16). Figure 17:  $^{13}\text{C}$  NMR spectrum (100 MHz;  $\text{CDCl}_3$ ) of (2-methoxy-8-methylquinolin-3-yl)methanol (16). Figure 18:  $^1\text{H}$  NMR (400 MHz;  $\text{CDCl}_3$ ) spectrum of (2-ethoxy-8-methylquinolin-3-yl)methanol (17). Figure 19:  $^{13}\text{C}$  NMR (100 MHz;  $\text{CDCl}_3$ ) spectrum of (2-ethoxy-8-methylquinolin-3-yl)methanol (17). (*Supplementary Materials*)

## References

- [1] K. D. Thomas, A. V. Adhikari, and N. S. Shetty, "Design, synthesis and antimicrobial activities of some new quinoline derivatives carrying 1,2,3-triazole moiety," *European Journal of Medicinal Chemistry*, vol. 45, no. 9, pp. 3803–3810, 2010.
- [2] O. Navneetha, K. Deepthi, A. Muralidha Rao, and T. Jyostn, "A review on chemotherapeutic activities of quinoline," *IJPCBS*, vol. 7, no. 4, pp. 364–372, 2017.
- [3] S. Poonam, K. Kamaldeep, C. Amit, S. Rran]dh, and R. Dhawan, "A review on biological activities of quinoline derivatives," *Journal of Management, Information Technology and Engineering*, vol. 2, no. 1, pp. 1–14, 2016.
- [4] M. Emmerson and A. Jnes, "The quinolones: decades of development and use," *Journal of Antimicrobial Chemotherapy*, vol. 51, pp. 13–20, 2003.
- [5] G. S. Bisacchi, "Origins of the quinolone class of antibacterials: an expanded "discovery story1," *Journal of Medicinal Chemistry*, vol. 58, no. 12, pp. 4874–4882, 2015.
- [6] P. Sharma, A. Jain, and S. Jain, "Fluoroquinolone antibacterials: a review on chemistry, microbiology and therapeutic prospects," *Acta Poloniae Pharmaceutica-Drug Research*, vol. 66, no. 6, pp. 587–604, 2009.
- [7] G. Sárközy, "Quinolones: a class of antimicrobial agents," *Veterinárni Medicina*, vol. 46, no. 9–10, pp. 257–274, 2001.
- [8] N. Riahifard, K. Tavakoli, J. Yamaki, K. Parang, and R. Tiwari, "Synthesis and evaluation of antimicrobial activity of [R4W4K]-Levofloxacin and [R4W4K]-Levofloxacin-Q conjugates," *Molecules*, vol. 22, no. 6, p. 957, 2017.
- [9] C. Y. Hong, "Discovery of gemifloxacin (Factive, LB20304a): a quinolone of new a generation," *Il Farmaco*, vol. 56, no. 1-2, pp. 41–44, 2001.
- [10] A. M. Farghaly, N. S. Habib, M. A. Khalil, O. A. El-Sayed, and A. E. Bistawroos, "Synthesis of novel 2-substituted quinoline derivatives: antimicrobial, inotropic, and chronotropic activities," *Archiv der Pharmazie*, vol. 323, no. 4, pp. 247–251, 1990.
- [11] B. Swamy, Y. Praveen, N. Pramod, B. Shivkumar, H. Shivkumar, and R. Rao, "Synthesis, characterization and anti-inflammatory activity of 3-formyl 2-hydroxy quinoline thiosemicarbazides," *Journal of Pharmacy Research*, vol. 5, no. 5, pp. 2735–2737, 2012.
- [12] N. Khalifa, M. Al-Omar, A. El-Galil, and M. El-Reheem, "Anti-inflammatory and analgesic activities of some novel carboxamides derived from 2-phenyl quinoline candidates," *Biomedical Research*, vol. 28, no. 2, pp. 869–874, 2017.
- [13] S. Gupta and A. Mishra, "Synthesis, characterization & screening for anti-inflammatory & analgesic activity of quinoline derivatives bearing azetidinone scaffolds," *Anti-Inflammatory & Anti-allergy Agents in Medicinal Chemistry*, vol. 15, no. 1, 2016.
- [14] X. Ngoro, N. Tobeka, and B. Aderibigbe, "Quinoline-based hybrid compounds with antimalarial activity," *Molecules*, vol. 22, no. 12, p. 2268, 2017.
- [15] S. Nara and A. Garlapati, "Design, Synthesis and molecular docking study of hybrids of quinazolin-4(3H)-one as anti-cancer agents," *Ars Pharmaceutica*, vol. 59, no. 3, pp. 121–131, 2018.
- [16] M. Bingul, O. Tan, C. Gardner et al., "Synthesis, characterization and anti-cancer activity of hydrazide derivatives incorporating a quinoline moiety," *Molecules*, vol. 21, no. 7, p. 916, 2016.
- [17] M. Zemtsova, A. Zimichev, P. Trakhtenberg, Y. Klimochkin et al., "Synthesis and antiviral activity of several quinoline derivatives," *Pharmaceutical Chemistry Journal*, vol. 45, no. 5, 2011.
- [18] M. Zemtsova, A. Zimichev, P. Trakhtenberg, R. Belen'kaya, and E. Boreko, "Synthesis and antiviral activity of 4-quinolinecarboxylic acid hydrazides," *Pharmaceutical Chemistry Journal*, vol. 42, no. 10, 2008.
- [19] P. Miniyar, M. Barmade, and A. Mahajan, "Synthesis and biological evaluation of 1-(5-(2-chloroquinolin-3-yl)-3-phenyl-1H-pyrazol-1-yl)ethanone derivatives as potential antimicrobial agents," *Journal of Saudi Chemical Society*, vol. 19, no. 6, pp. 655–660, 2014.
- [20] P. G. Mandhane, R. S. Joshi, P. S. Mahajan, M. D. Nikam, D. R. Nagargoje, and C. H. Gill, "Synthesis, characterization and antimicrobial screening of substituted quiazolinones derivatives," *Arabian Journal of Chemistry*, vol. 8, no. 4, pp. 474–479, 2015.
- [21] A. Ansari, S. Ahmed, M. Waheed, and A. Juned, "Extraction and determination of antioxidant activity of Withania somnifera Dunal," *European Journal of Experimental Biology*, vol. 3, no. 5, pp. 502–507, 2013.
- [22] O. Trott and A. J. Olson, "AutoDock Vina: improving the speed and accuracy of docking with a new scoring function, efficient optimization, and multithreading," *Journal of Computational Chemistry*, vol. 31, no. 2, pp. 455–461, 2010.
- [23] S. Narramore, C. E. M. Stevenson, A. Maxwell, D. M. Lawson, and C. W. G. Fishwick, "New insights into the binding mode of pyridine-3-carboxamide inhibitors of *E. coli* DNA gyrase," *Bioorganic & Medicinal Chemistry*, vol. 27, no. 16, pp. 3546–3550, 2019.
- [24] D. Seeliger and B. L. de Groot, "Ligand docking and binding site analysis with PyMOL and Autodock/Vina," *Journal of Computer-Aided Molecular Design*, vol. 24, no. 5, pp. 417–422, 2010.

- [25] R. Ziraldo, A. Hanke, and S. D. Levene, "Kinetic pathways of topology simplification by Type-II topoisomerases in knotted supercoiled DNA," *Nucleic Acids Research*, vol. 47, no. 1, pp. 69–84, 2019.
- [26] C. J. Dorman and M. J. Dorman, "DNA supercoiling is a fundamental regulatory principle in the control of bacterial gene expression," *Biophysical Reviews*, vol. 8, no. 3, pp. 209–220, 2016.
- [27] A. J. Schoeffler and J. M. Berger, "DNA topoisomerases: harnessing and constraining energy to govern chromosome topology," *Quarterly Reviews of Biophysics*, vol. 41, no. 1, pp. 41–101, 2008.
- [28] Z. Jakopin, J. Ilas, M. Barancokova et al., "Discovery of substituted oxadiazoles as a novel scaffold for DNA gyrase inhibitors," *European Journal of Medicinal Chemistry*, vol. 130, pp. 171–184, 2017.